




Retinal Biomarkers Discovery for Cerebral Small Vessel Disease in an Older Population

Lucia Ballerini¹(✉) , Ahmed E. Fetit², Stephan Wunderlich¹,
Ruggiero Lovreglio³, Sarah McGrory¹, Maria Valdes-Hernandez¹,
Tom MacGillivray¹, Fergus Doubal¹, Ian J. Deary⁴, Joanna Wardlaw¹,
and Emanuele Trucco²

¹ Department of Neuroimaging Sciences, Centre for Clinical Brain Sciences,
and VAMPIRE Project, University of Edinburgh, Edinburgh, UK

lucia.ballerini@ed.ac.uk

² VAMPIRE Project, CVIP, Computing (SSE), University of Dundee, Dundee, UK

³ School of Built Environment, Massey University, Auckland, New Zealand

⁴ Centre for Cognitive Ageing and Cognitive Epidemiology, University of Edinburgh,
Edinburgh, UK

Abstract. The retinal and cerebral microvasculatures share many morphological and physiological properties. In this pilot we study the strength of the associations between morphological measurements of the retinal vasculature, obtained from fundus camera images, and of features of Small Vessel Disease (SVD), as white matter hyperintensities (WMH) and perivascular spaces (PVS), obtained from MRI brain scans. We performed a 500-trial bootstrap analysis with Regularized Gaussian linear regression on a cohort of older community-dwelling subjects (Lothian Birth Cohort 1936, $N = 866$) in their eighth decade. Arteriolar bifurcation coefficients, vessel tortuosity and fractal dimension predicted WMH volume in 23% of the trials. Arteriolar widths, venular bifurcation coefficients, and venular tortuosity predicted PVS in up to 99.6% of the trials.

Keywords: Small vessel disease · Retina · Biomarkers

1 Introduction

Small Vessel Diseases (SVDs) are a group of disorders that result from pathological alteration of the small blood vessels in the brain, including the small arteries, capillaries and veins. Of the about 36 million people that are estimated to suffer from dementia worldwide, up to 65% have an SVD component. Furthermore, SVD causes about 25% of strokes, worsens outcome after stroke and is a leading cause of disability, cognitive impairment and poor mobility [5].

Due to the developmental, anatomical and physiological similarities of the cerebral and retinal vessels [20], and the ease with which the retinal microvasculature can be imaged *in vivo*, there has been considerable interest in determining whether pathologic changes in the retinal vessels parallel changes in cerebral

vascular health, in particular in SVD [1, 9, 15]. Morphological features of the retinal vasculature have been associated with stroke, especially small vessel disease (lacunar) stroke [8, 9]. Arteriolar branching coefficients of retinal vessels have also been associated with periventricular and deep white matter hyperintensities (WMH) [7]. Reduced fractal dimension (a measure of the complexity of the retinal vascular network) in older people has been related to WMH severity and total SVD burden [16]. Narrower retinal arteriolar calibre has been related to more visible perivascular spaces (PVS) on brain magnetic resonance imaging (MRI) [19]. Here we consider an array of retinal measurements in an effort to identify those most closely related to two main features of SVD: WMH and PVS, both quantified with computational methods reported elsewhere [2, 24].

We present results of a bootstrap analysis with Regularized Gaussian linear regression and cross-validation in a cohort of older community-dwelling subjects in their eighth decade. This analysis determines which retinal feature sets are selected most often in building sparse linear regression models, indicating their importance in predicting associations with WMH and PVS. We report findings from experiments with and without demographics and common vascular factors (VRF) as covariates, along with retinal measurements.

2 Materials and Methods

2.1 Study Population

We used data from a sample of the Lothian Birth Cohort 1936 (LBC1936) [6, 21], a community-dwelling cohort being studied in the eighth decade of life. The LBC1936 comprises 1091 individuals survivors of the Scottish Health Survey of 1947, who were recruited into the study at the age of 70. Of these, 866 were tested at the second wave of recruitment, at mean age 72.55 years (SD 0.71), of whom 700 had structural MRI scans, and 814 had fundus photography of both eyes. Experiments were based on subjects with retinal and MRI data that could be processed successfully, resulting in 478 and 381 subjects for WMH and PVS, respectively.

All participants gave written informed consent under protocols approved by the Lothian (REC 07/MRE00/58) and Scottish Multicentre (MREC/01/0/56) Research Ethics Committees (<http://www.lothianbirthcohort.ed.ac.uk/>).

All clinical and imaging acquisition methods in this cohort have been reported previously [6, 21, 25]. Medical history variables (hypertension, diabetes, hypercholesterolemia, cardiovascular disease history (CVD)) were assessed at the same age as brain imaging.

2.2 Retinal Measurements

Digital retinal fundus images were captured using a non-mydratic camera at 45° field of view (CRDGi; Canon USA, Lake Success, New York, USA). All images were centred on the optic disc [18]. Retinal vascular measurements were

computed for both eyes of each of the included participants using the semi-automated software package, VAMPIRE (Vessel Assessment and Measurement Platform for Images of the REtina, University of Edinburgh and Dundee, UK) version 3.1 [22,23] (Fig. 1), by a trained operator blinded to all other data.

Image rejection was decided by operator inspection (e.g. not enough vessels visible) or not being able to complete the analysis. Reasons for rejecting image included poor image quality (e.g. significant blur or cataract obscuring the view of the retina) and lesions compromising the vasculature appearance preventing adequate segmentation for subsequent vessel analysis. Subjects were excluded if images of one or both eyes were unsuitable for analysis.

VAMPIRE 3.1 computes 151 morphometric measurements of the retinal vasculature for each eye, yielding to a total of 302 features per subject, including standard measurements in Zone B and C (Fig. 1), i.e. central retinal artery equivalent (CRAE), central retinal vein equivalent (CRVE), arteriole-to-venule ratio (AVR), arteriolar and venular fractal dimension (D0a, D0v) and tortuosity estimates, described in details in Material of [16]. Measurements of each type above are computed by vessel type (artery or vein), zone, quadrant and vessel generation.

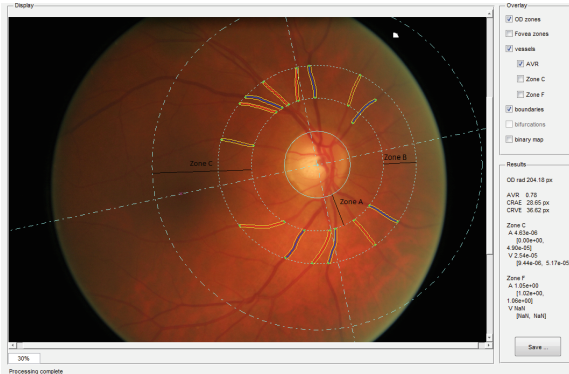


Fig. 1. Retinal fundus image with vessel segments computed in Zone B. Solid lines (red for arterioles and dark blue for venules) represent the vessels detected automatically and measured by VAMPIRE. Dotted lines trace the vessels contours computed. (Color figure online)

2.3 Brain Imaging

Structural brain MRI data were acquired using a 1.5-Tesla GE Signa Horizon HDx scanner (General Electric, Milwaukee, WI), with coronal T1-weighted (T1w), and axial T2-weighted (T2w), T2*-weighted (T2*w) and fluid-attenuated inversion recovery (FLAIR)-weighted whole-brain imaging sequences. See [25] for details.

Intracranial Volume (ICV) and WMH volume were measured on T2w, T1w, T1*w and FLAIR scans using a validated semi-automatic pipeline, based on a multispectral data fusion, reported elsewhere [24]. For this study we express WMH as percentage of ICV.

The computational assessment of PVS used the T2w images acquired with 11,320 ms repetition time, 104.9 ms echo time, 20.83 KHz bandwidth and 2 mm slice thickness. The images were reconstructed to a $256 \times 256 \times 80$ matrix, 1 mm in-plane resolution. PVS were segmented in the centrum semiovale with the method described in [2]. Briefly the PVS computational method uses the three-dimensional Frangi filter [12], which parameters are optimized as described in [2], to enhance and capture the 3D geometrical shape of PVS. Images were checked and deemed acceptable according to quality control criteria reported elsewhere [3]. The PVS total volume was the total number of voxels classified as PVS. An example of WMH and PVS segmentation is shown in Fig. 2.

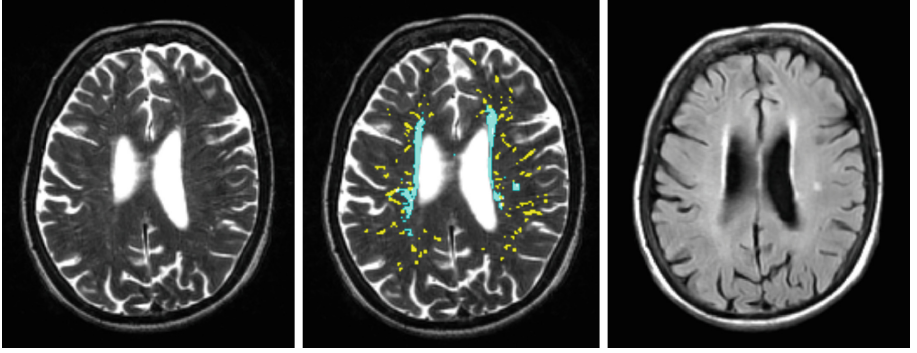


Fig. 2. Example of brain lesion segmentation: axial T2-weighted slice showing detected WMH in cyan and PVS in yellow. Corresponding source T2-weighted (left) and FLAIR (right). (Color figure online)

2.4 Biomarker Discovery by Regularized Gaussian Regression

Our method is based on the framework reported in [11], with the modifications described here. Gaussian linear regression was used for ease of model interpretation; model coefficients can be directly linked to feature importance. Regularization was used to perform shrinkage and promote sparsity. This approach is well suited for biomarkers identification as it performs feature selection and model estimation simultaneously. Assume we have vectors of observations, $\mathbf{x}_i \in \mathbf{R}^p$, and the corresponding likelihoods for each class $y_i \in \mathbf{R}$, $i = 1, \dots, N$. The Elastic Net [26] objective function for the Gaussian family is:

$$\min_{(\beta_0, \beta) \in \mathbf{R}^{p+1}} \frac{1}{2N} \sum_{i=1}^N (y_i - \beta_0 - \mathbf{x}_i^T \beta)^2 + \lambda[(1 - \alpha)\|\beta\|_2^2/2 + \alpha\|\beta\|_1], \quad (1)$$

where β_0 and $\beta = [\beta_1, \beta_2, \dots, \beta_p]$ are the regression model coefficients, $\lambda \geq 0$ controls the strength of regularization and the elastic next regularization parameter $0 \leq \alpha \leq 1$ quantifies the compromise between ridge ($\alpha = 0$) and lasso ($\alpha = 1$). For highly correlated features, the lasso tends to pick one of the features and discard the others (promoting sparsity, hence identifying the most relevant features), whereas the ridge shrinks the feature coefficients towards each other.

The R package *glmnet* [13] was used to perform the regularized linear regression experiments. Cross-validation was used to select λ . Two values of interest are reported by *glmnet*: λ_{min} , the value of λ at which the lowest validation set error is achieved, and λ_{1SE} , the λ for the model for which the validation error is within one standard error of λ_{min} .

We report experiments using lasso and λ_{min} , that drive some model coefficients to zero and thus perform feature selection. As different data samples give rise to different feature sets being selected, we perform a bootstrap analysis, measuring how likely features and feature subsets are to be included in the models for randomly chosen data samples. The bootstrap has been shown useful in addressing the lasso issues of data dependency and instability [10]. Each bootstrap analysis comprised 500 bootstrap trials.

We performed 4 sets of experiments, using WMH and PVS as outcome (see Table 1). We used two feature vectors: one including VAMPIRE measurements only, the other VAMPIRE measurements and gender, age at scan, and vascular risk factors (hypertension, diabetes, hypercholesterolemia and CVD). Model selection used 10-fold cross-validation (CV) to choose λ . The feature coefficients (β) computed were recorded for each λ value (e.g. λ_{min}). We then computed the number of times (frequency) within the 500 bootstraps that each feature had a non-zero weight, reflecting its importance for a specific model in the bootstrap protocol.

Table 1. Sets of experiments

Experiment name	Predictors	Outcome
WMH _{Retina}	Retina	WMH
WMH _{Retina&VRF}	Retina & VRF	WMH
PVS _{Retina}	Retina	PVS
PVS _{Retina&VRF}	Retina & VRF	PVS

3 Results

Figure 3 and 4 show examples of a bootstrap trial with outcomes WMH and PVS, respectively. As can be observed, reduced numbers of features reduce the mean squared error, suggesting that, for this data set, a small feature set is comparatively very important.

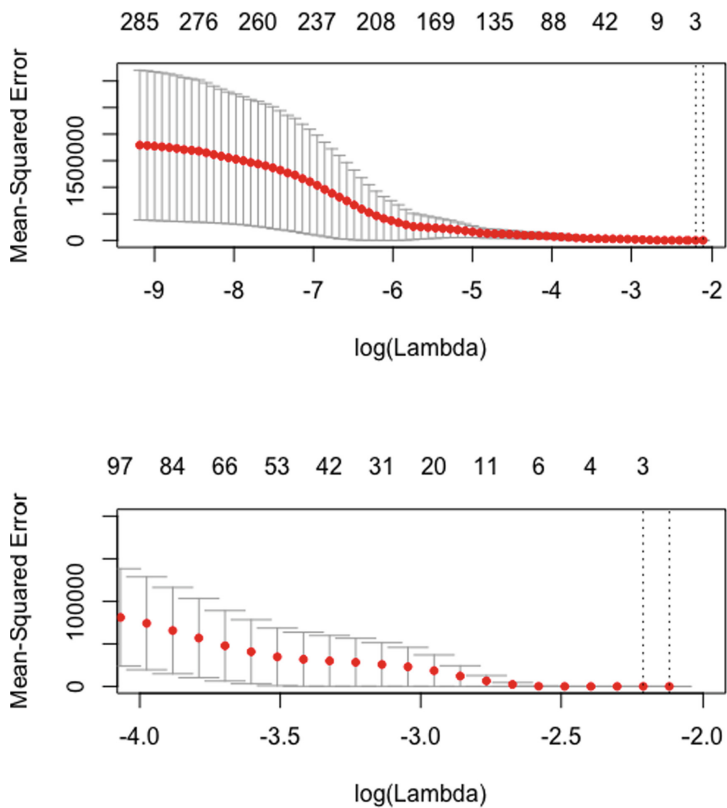


Fig. 3. Example of an individual bootstrap trial with WMH as outcome. Varying λ affects the Mean-Squared-Error (with 10-fold CV). Numbers above figure are the numbers of features retained in the regularized model. Interval bars are standard deviations. Bottom image is a zoom of the last part of the top one

Table 2 shows the results of the 4 experiments with different combinations of predictors (retinal features alone or retinal features plus others) and outcome (WMH or PVS volume). As can be seen in the table different retinal features were chosen for different outcomes, while the same retinal features were selected when VRF were included or not as predictors. In the experiments with WMH as outcome only hypertension was selected among the VRF.

3.1 Findings

In this specific cohort, increased arteriolar tortuosity, decreased arteriolar branching coefficients and decreased arteriolar fractal dimension were the strongest predictors of increased WMH volume. These predictors survived when we included VRF in the model. In this case, hypertension was also selected. Retinal measurements were selected in 117/500 trials (23.4%) in the first set of

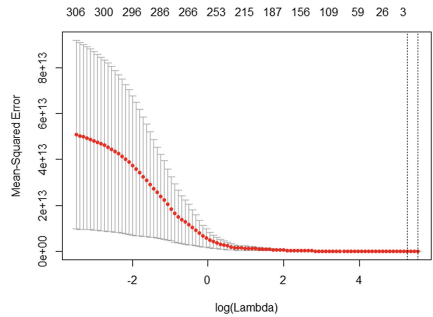


Fig. 4. Example of an individual bootstrap trial with PVS as outcome. Varying λ affects the Mean-Squared-Error (with 10-fold CV). Numbers above figure are the numbers of features retained in the regularized model. Interval bars are standard deviations

Table 2. Relative feature importance as the number of times a feature was selected (non-zero weight) in the 500 bootstraps, and direction of associations (+/- sign), for the 4 sets of experiments described in Table 1. Note: TortG1a = arteriolar tortuosity, BCa = arteriolar branching coefficients, D0a = fractal dimension of the arterial vasculature, GradQ3a = gradient of width of the main arteriole, BSTDa = standard deviation of the arteriole widths, TortQ4G1v = venular tortuosity, GradQ4a = gradient of width of the main arteriole, GradQ4a = gradient of width of the main venule, CRAE = central retinal arterial equivalent, BCv = venular branching coefficients, TortQ3v = venular tortuosity.

Features	WMH _{Retina}	WMH _{Retina&VRF}	Features	PVS _{Retina}	PVS _{Retina&VRF}
TortG1a	117 +	102 +	CRAE	498 -	498 -
BCa	117 -	102 -	BCv	484 +	484 +
D0a	117 -	102 -	TortQ3v	322 +	322 +
GradQ3a	61 +	77 +			
BSTDa	34 +	52 +			
TortQ4G1v	10 +	21 +			
GradQ4a		4 +			
GradQ3v		4 +			
Hibp		95 +			
age		4 +			
gender		4 +			

experiments, and in 102/500 trials (22.4%) in the second set. Decreased CRAE, increased venular bifurcation coefficients, and increased venular tortuosity were selected as predictors of increased PVS volume. These features were selected in 498, 484, 322 trials (99.6%, 96.8%, 64.4%) respectively.

4 Discussion and Conclusions

This pilot study used a bootstrap analysis based on regularized Gaussian linear regression and bootstrap to investigate the associations or retinal vascular fea-

tures computed with VAMPIRE 3.1 software in fundus camera images compared with WMH and PVS as outcomes in older people.

Our findings are in agreement with those of several previous clinical and population-based studies that showed associations between retinal vascular changes and markers of cerebral small vessel disease; see Hilal et al. [14] for a useful summary. For instance, Mutlu et al. [19] reported associations between retinal vessel width and PVS using visual rating scales. Using our same cohort, McGrory et al. [16] reported significant associations between fractal dimension and WMH. Doubal et al. [7] reported associations between bifurcation coefficients and WMH in patients presenting with mild stroke.

The present findings support the hypothesis that retinal fractal dimension is a possible indicator of the state of health of the brain vasculature and might have a significant associations with changes taking place in cerebral small vessels. Reduced branching coefficients were also associated with more WMH. The relationship between tortuosity and SVD may reflect worsening vessel wall contractility. Since both arteriole narrowing is an indicator of adverse microvessel health, this work provides further evidence that increase in total visible PVS volume reflect underlying microvascular pathology rather than being an epiphenomenon.

4.1 Strengths, Limitations and Future Work

The strengths of the current study include the use of computational measures which increase sensitivity respect to previous studies that used visual scores [16,19]. Furthermore, compared with previous studies, we have looked simultaneously at a wider range of key retinal vascular characteristics so as to sort out the relative importance of each. To our knowledge, the current study is the first that uses regularized regression to investigate the strength of retinal measurements to associate with computational measure of WMH and PVS.

This study has several limitations. First, its cross-sectional design preventing us from estimating the role of retinal parameters for risk prediction. Longitudinal studies examining retinal changes and progression of WMH and PVS would be valuable to assess retinal features as actual *predictors* of worsening WMH and PVS and as early manifestation of SVD. Such cohorts are not easily accessible at the time of writing. Second, it was possible to obtain valid quantitative measurements (retina and brain) only in a subset of the sample (68%). Future work includes developing feature measuring algorithms resilient to image variations [4]. Third, the quantitative effect on statistical inference of inaccuracies in the semi-automatic measurements of the retinal vasculature has never been modelled. For instance, CRAE and CRVE are subject to magnification effects and refractive error; FD is dependent on the vessel segmentation accuracy, which in turn depends on image quality, presence of cataracts and floaters [17]. Fourth, results were obtained with 10-fold cross-validation; a held-out test set could be adopted to improve performance, although the focus of this work was investigating discriminative sets of retinal features, not maximizing performance.

Acknowledgements. The LBC1936 Study (<http://www.disconnectedmind.ed.ac.uk/>) was funded by Age UK and the UK Medical Research Council (MR/R02462/1, MR/013111/1, G1001245, Ref. 82800) (including the Sidney De Haan Award for Vascular Dementia). Funds were also received from The University of Edinburgh Centre for Cognitive Ageing and Cognitive Epidemiology, part of the cross council Lifelong Health and Wellbeing Initiative (MR/K026992/1), and the Biotechnology and Biological Sciences Research Council (BBSRC). The work was also funded by the EPSRC grant [LB EP/M005976/1], the Fondation Leducq Network for the Study of Perivascular Spaces in Small Vessel Disease [LB 16 CVD 05], the Row Fogo Charitable Trust [MVH Grant No. BROD.FID3668413], the European Union Horizon 2020 [PHC-03-15, project No 666881, “SVDs@Target”], the UK Dementia Research Institute at the University of Edinburgh and the British Heart Foundation Centre for Research Excellence, Edinburgh.

References

1. Arboix, A.: Retinal microvasculature in acute lacunar stroke. *Lancet Neurol.* **8**(7), 596–598 (2009). [https://doi.org/10.1016/S1474-4422\(09\)70137-1](https://doi.org/10.1016/S1474-4422(09)70137-1)
2. Ballerini, L., et al.: Perivascular spaces segmentation in brain MRI using optimal 3D filtering. *Sci. Rep.* **8** (2018). <https://doi.org/10.1038/s41598-018-19781-5>
3. Ballerini, L., et al.: Computational quantification of brain perivascular space morphologies: Associations with vascular risk factors and white matter hyperintensities. a study in the lothian birth cohort 1936. *NeuroImage: Clinical* **25**, 102120 (2020). <https://doi.org/10.1016/j.nicl.2019.102120>
4. Bernal, J., et al.: Retrospective imaging artefact reduction improves perivascular spaces segmentation and quantification in brain magnetic resonance imaging. In: *Medical Image Understanding and Analysis*. Springer International Publishing (2020)
5. Brown, R., et al.: Understanding the role of the perivascular space in cerebral small vessel disease. *Cardiovascular Research*, p. cvy113 (2018). <https://doi.org/10.1093/cvr/cvy113>
6. Deary, I.J., et al.: The Lothian Birth Cohort 1936: a study to examine influences on cognitive ageing from age 11 to age 70 and beyond. *BMC Geriatr.* **7**, 28–28 (2007). <https://doi.org/10.1186/1471-2318-7-28>
7. Doubal, F.N., et al.: Retinal arteriolar geometry is associated with cerebral white matter hyperintensities on magnetic resonance imaging. *Int J. Stroke* **5**(6), 434–439 (2010). <https://doi.org/10.1111/j.1747-4949.2010.00483.x>
8. Doubal, F.N., Hokke, P.F., Wardlaw, J.M.: Retinal microvascular abnormalities and stroke: a systematic review. *J. Neurol. Neurosurg. Psychiatry* **80**(2), 158–165 (2009). <https://doi.org/10.1136/jnnp.2008.153460>
9. Dumitrascu, O.M., et al.: Retinal microvascular abnormalities as surrogate markers of cerebrovascular ischemic disease: a meta-analysis. *J. Stroke Cerebrovasc. Dis. off. J. Natl. Stroke Assoc.* **27**(7), 1960–1968 (2018). <https://doi.org/10.1016/j.jstrokecerebrovasdis.2018.02.041>
10. Efron, B., Tibshirani, R.J.: An Introduction to the Bootstrap. No. 57 in *Monographs on Statistics and Applied Probability*. Chapman & Hall/CRC, Boca Raton (1993)
11. Fetit, A.E., et al.: A multimodal approach to cardiovascular risk stratification in patients with type 2 diabetes incorporating retinal, genomic and clinical features. *Sci. Rep.* **9**(1), 3591 (2019). <https://doi.org/10.1038/s41598-019-40403-1>

12. Frangi, A., Niessen, W., Vincken, K., Viergever, M.: Multiscale vessel enhancement filtering. In: Medical Image Computing and Computer-Assisted Intervention (MICCAI98), pp. 130–137 (1998). <https://doi.org/10.1007/BFb0056195>
13. Friedman, J., Hastie, T., Tibshirani, R.: Regularization paths for generalized linear models via coordinate descent. *J. Stat. Softw.* **33**(1), 1–22 (2010). <https://doi.org/10.18637/jss.v033.i01>
14. Hilal, S., et al.: Microvascular network alterations in retina of subjects with cerebral small vessel disease. *Neurosci. Lett.* **577**, 95–100 (2014). <https://doi.org/10.1016/j.neulet.2014.06.024>
15. Lindley, R.I.: Retinal microvascular signs: a key to understanding the underlying pathophysiology of different stroke subtypes? *Int. J. Stroke* **3**(4), 297–305 (2008). <https://doi.org/10.1111/j.1747-4949.2008.00215.x>
16. McGrory, S., et al.: Retinal microvasculature and cerebral small vessel disease in the Lothian Birth Cohort 1936 and Mild Stroke Study. *Sci. Rep.* **9**(1), 6320–6320 (2019). <https://doi.org/10.1038/s41598-019-42534-x>
17. McGrory, S., et al.: Towards standardization of quantitative retinal vascular parameters: comparison of SIVA and VAMPIRE measurements in the Lothian Birth Cohort 1936. *Transl. Vis. Sci. Technol.* **7**(2), 12 (2018). <https://doi.org/10.1167/tvst.7.2.12>
18. Mookiah, M.R.K., et al.: Towards standardization of retinal vascular measurements: on the effect of image centering. In: Stoyanov, D., et al. (eds.) OMIA/COMPAY -2018. LNCS, vol. 11039, pp. 294–302. Springer, Cham (2018). https://doi.org/10.1007/978-3-030-00949-6_35
19. Mutlu, U., et al.: Retinal microvascular calibers are associated with enlarged perivascular spaces in the brain. *Stroke* **47**(5), 1374–1376 (2016). <https://doi.org/10.1161/strokeaha.115.012438>
20. Patton, N., Aslam, T., Macgillivray, T., Pattie, A., Deary, I., Dhillon, B.: Retinal vascular image analysis as a potential screening tool for cerebrovascular disease: a rationale based on homology between cerebral and retinal microvasculatures. *J. Anat.* **206**(4), 319–348 (2005). <https://doi.org/10.1111/j.1469-7580.2005.00395.x>
21. Taylor, A.M., Pattie, A., Deary, I.J.: Cohort profile update: The Lothian Birth Cohorts of 1921 and 1936. *Int. J. Epidemiol.* **47**(4), 1042–1042r (2018). <https://doi.org/10.1093/ije/dyy022>
22. Trucco, E., et al.: Novel VAMPIRE algorithms for quantitative analysis of the retinal vasculature. In: 2013 ISSNIP Biosignals and Biorobotics Conference: Biosignals and Robotics for Better and Safer Living (BRC), pp. 1–4 (2013). <https://doi.org/10.1109/BRC.2013.6487552>
23. Trucco, E., et al.: Morphometric measurements of the retinal vasculature in fundus images with VAMPIRE. *Biomedical Image Understanding*, pp. 91–111 (2015)
24. Valdés-Hernández, M.d.C., Ferguson, K.J., Chappell, F.M., Wardlaw, J.M.: New multispectral MRI data fusion technique for white matter lesion segmentation: method and comparison with thresholding in FLAIR images. *Eur. Radiol.* **20**(7), 1684–1691 (2010). <https://doi.org/10.1007/s00330-010-1718-6>
25. Wardlaw, J.M., et al.: Brain aging, cognition in youth and old age and vascular disease in the Lothian Birth Cohort 1936: rationale, design and methodology of the imaging protocol. *Int. J. Stroke* **6**(6), 547–559 (2011). <https://doi.org/10.1111/j.1747-4949.2011.00683.x>
26. Zou, H., Hastie, T.: Regularization and variable selection via the elastic net. *J. Roy. Stat. Soc. Ser. B (Statistical Methodology)* **67**(2), 301–320 (2005)